Frontiers in Heat and Mass Transfer (FHMT), 4, 013002 (2013)
DOI: 10.5098/hmt.v4.1.3002

Global Digital Central
ISSN: 2151-8629

Frontiers in Heat and Mass Transfer

Available at www.ThermalFluidsCentral.org

INVESTIGATION OF PARTICULAR FEATURES OF THE NUMERICAL SOLUTION OF AN EVAPORATING THIN FILM IN A CHANNEL

Greg Ball, John Polansky, Tarik Kaya*

Department of Mechanical and Aerospace Engineering, Carleton University, Ottawa, Ontario, K1S 5B6, Canada

ABSTRACT

The fluid flow and heat transfer in an evaporating extended meniscus are numerically studied. Continuity, momentum, energy equations and the Kelvin-Clapeyron model are used to develop a third order, non-linear ordinary differential equation which governs the evaporating thin film. It is shown that the numerical results strongly depend on the choice of the accommodation coefficient and Hamaker constant as well as the initial perturbations. Therefore, in the absence of experimentally verified values, the numerical solutions should be considered as qualitative at best. It is found that the numerical results produce negative liquid pressures under certain specific conditions. This result may suggest that the thin film can be in an unstable state of tension; however, this finding remains speculative without experimental validation. Although similar thin-film models proved to be very useful in gaining qualitative insight into the characteristics of evaporating thin films, the results shown in this study indicate that careful experimental investigations are needed to verify the mathematical models.

Keywords: *Thin film, evaporating meniscus, capillary force, disjoining pressure*

1. INTRODUCTION

The study of thin films is important in many technological applications, including the cooling of electronics, evaporation, condensation, boiling, drying etc. The film dynamics are governed by various complex physical mechanisms such as surface tension, disjoining pressure, thermal conduction and phase change. Because of its importance, thin films have been widely studied.

The problem of modelling an evaporating thin film has been investigated by many authors using various techniques. Solutions governed by 3rd and 4th order Ordinary Differential Equations (ODE) have been proposed. In addition to the problem formulation (3rd versus 4th order), the existing models used different boundary conditions, and different techniques in the calculation of the mass transport across the interface. More recently, simulations based on the molecular dynamics were also attempted. Because of the very small length scales involved, few experimental works have been completed and majority of the models do not have the necessary validation required for providing further insight into whether the models produce accurate physical solutions.

Several authors have expanded upon current works by imposing different boundary conditions and observing the corresponding effect. Table 1 provides a sample of common variations undertaken by various authors. Note that the varying thermophysical properties, refers to whether the numerical model updates the fluid properties as a function of temperature in generating a solution.

Table 1 Comparison of some earlier works on modelling an evaporating meniscus.

Authors	Non-isothermal Interfacial Condition	Varying Thermophysical Properties	Slip Boundary condition	Polarity Effect	Superheat Effect (at least 5 K range)
Potash and Wayner (1972)	✓	-	-	-	-
Wayner et al. (1976)	✓	-	-	-	-
Moosman and Homsy (1980)	✓	-	-	-	-
Hallinan et al. (1994)	✓	-	-	-	-
Park et al. (2003)	-	-	✓	-	-
Qu et al. (2002)	✓	-	-	✓	-
Zhao et al. (2011)	✓	✓	-	-	✓
Wee et al. (2005)	✓	✓	✓	✓	-
Wang et al. (2007)	✓	-	-	-	✓
Present Study	✓	✓	✓	-	✓

* *Corresponding author. E-mail: tkaya@mae.carleton.ca.*

DOI: 10.5098/hmt.v4.1.3002 ISSN: 2151-8629

Of the parameters listed on Table 1, the following general trends were observed. Potash and Wayner (1972) were the first to show that both pressure gradient and evaporative mass flux reach a maximum within the thin-film region. Moosman and Homsy (1980) implemented a mathematical model to describe the thin-film characteristics using perturbation analysis. The effect of including an interfacial temperature gradient term, as well as varying thermophysical properties allowed for much more pronounced effects to be seen when superheat is varied (Zhao et al., 2011). An increased superheat serves to lessen the adsorbed film thickness, and creates a much more aggressive curvature increase as the film transitions from the adsorbed region through the thin-film region. In general, for higher superheats the film length is decreased, creating a much 'steeper' thin-film profile (Zhao et al., 2011). When polar effects were considered on the disjoining pressure model, the thin-film length was extended, all the while reducing the evaporative heat transfer (Wee et al., 2005). The wall slip boundary condition as introduced by Park et al. (2003), serves to elongate the thin film while yielding a lower pressure gradient (Wee et al., 2005).

In addition to the above trends, variance in channel width has also been studied, such as in Wang et al. (2007). The effect of an increasing channel width, was an increased thin-film length (Qu et al. 2002; Zhao et al., 2011). Du and Zhao (2012) attempted to quantify the effects of using altered evaporation models. They concluded that neglecting disjoining pressure terms have less of an effect than neglecting capillary pressure terms. They also concluded that the substrate thickness does have a minor effect on the total heat transfer.

Kou and Bai (2011) related wall slip to a temperature jump at the solid-liquid interface. They concluded that the presence of a temperature jump at the interface can reduce heat and mass transport characteristics.

It is important to mention that in the above works, solution methodology is similar. As such, the governing ODE is found to have a highly non-linear characteristic behaviour, regardless of order. If the initial conditions, such as slope and curvature, are assigned values of zero in the beginning of the thin film as one would assume, a constant thickness thin-film solution is obtained. As a result, perturbations must be applied in order to obtain a physical solution of interest. Considering the highly non-linear behaviour, it is difficult to identify a set of suitable perturbations that will yield a satisfactory solution. Most published works did not include their applied perturbations. Du and Zhao (2012) stated that the thickness perturbation, ε_1, should be set sufficiently close to zero and the slope perturbation, ε_2, should be set slightly larger than zero. Furthermore, altering parameters of the problem alters boundary conditions, which in turn have a profound effect on the perturbations. The solutions are also extremely sensitive to boundary conditions as noted in DasGupta et al. (1993).

Of note is the lack of relationship between the derivative perturbations and the magnitude of the applied superheat or channel width (Wang et al., 2007 and 2008; Park et al., 2003). These are not the only parameters that have an effect on applied perturbation. This research also notes extreme sensitivities to the slope perturbation, ε_2, as accommodation coefficient is altered.

Panchamgam et al. (2008) is the only work where the high-resolution data for thickness, slope and curvature were experimentally obtained and used as inputs to a macro-micro numerical model. Thus, the thin-film characteristics of a constrained vapour bubble - such as interfacial temperature profile, evaporative heat and mass flux – were directly calculated.

Morris (2003) presented a different and more rigorous approach to the same problem by matching the asymptotic solutions. He pointed out that the above methods divide the meniscus at an arbitrarily chosen point: nonlinear small region close to the apparent contact angle and relatively undisturbed region determined from the hydrostatics. In this work, it was shown that the above methods implicitly assume that the capillary number ($Ca = \mu V/\sigma$) of the induced flow is small.

In addition to the points raised by Morris (2003), we also identified that effects of certain variables often overlooked in these solutions, including the accommodation coefficient and Hamaker constant. It was found that these variables play a large role in the resulting thin-film characteristics.

In this paper, a mathematical model based on the augmented Young-Laplace and Kelvin-Clapeyron equations is studied. The main goal of our study is to investigate the effects of various parameters and identify the limits of the mathematical model in order to better understand the thin-film dynamics. A deliberate attempt is made to list the various parameters of the solution such as perturbations imposed and discuss in detail the validity limit of the solutions.

2. MATHEMATICAL MODEL

The meniscus is confined by a narrow channel with immiscible walls and of infinite depth, as illustrated in Fig. 1. The model developed herein, describes a thin film of non-polar fluid, evaporating in a steady-state condition, for a given superheat. The model proposed, follows a similar approach used in previous related works, e.g. Wee et al. (2005) and Panchamgam et al. (2008).

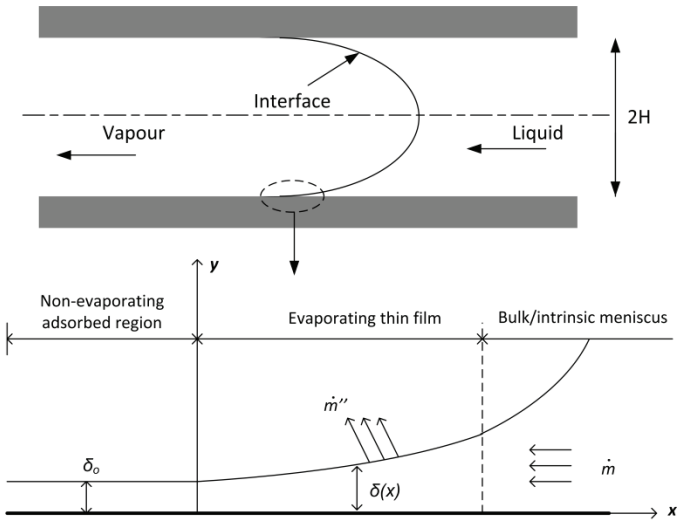

Fig. 1 Meniscus as it contacts a rigid and planar immiscible substrate.

The evaporating thin-film region of a meniscus is governed by the augmented Young-Laplace equation, as proposed by Wayner Jr. (1991), where the vapour pressure field is assumed uniform and constant.

$$P_v = P_l + P_d + P_c \tag{1}$$

The vapour pressure is balanced by the liquid, disjoining and capillary pressures found in the thin-film region. Of these pressures, the disjoining pressure for a pure, non-polar fluid is expressed as a function of the dispersion constant, A, and film thickness, δ, as follows

$$P_d = \frac{A}{\delta^3} \tag{2}$$

The dispersion constant, A, is related to the Hamaker constant, A_H, by the following relation: $A = A_H/6\pi$. Note that in some works both terms were alternatively used for the same value, leading to confusion in reproducing the results. The importance of the Hamaker

constant and its effect on the results will be discussed later in the paper.

The capillary pressure is expressed as the product of the surface tension and the local curvature. The surface tension is assumed to vary linearly with the local interfacial temperature.

$$P_c = \sigma\kappa \tag{3}$$

where,

$$\sigma = a + bT_{lv} \tag{4}$$

$$\kappa = \frac{\delta''}{\left(1+\delta'^2\right)^{3/2}} = \frac{\delta''}{\alpha^{3/2}} \tag{5}$$

Combining Eqs. (1-5) and differentiating with respect to *x*, the following third-order differential equation is obtained.

$$\delta''' = \frac{3\delta'\delta''^2}{\alpha} + \frac{\alpha^{3/2}}{\sigma}\left(\frac{3A}{\delta^4}\delta' - \frac{dP_l}{dx}\right) - \frac{b}{\sigma}\left(\frac{dT_{lv}}{dx}\right)\delta'' \tag{6}$$

Equation (6) captures the pressure gradient and thermocapillary effects present in the thin film. Both the liquid pressure and interfacial temperature gradients are needed to solve the governing equation.

As the film is evaporating, fluid must flow into the thin-film region from the bulk meniscus, so as to maintain steady state. The flow field in the thin-film liquid is solved with the use of the lubrication approximation, given by Eq. (7) and associated boundary conditions at the wall, Eq. (8), and the liquid-vapour interface, Eq. (9).

$$\frac{dP_l}{dx} = \mu\frac{d^2u}{dy^2} \tag{7}$$

$$u = -\beta\frac{du}{dy} \tag{8}$$

$$\tau = \sigma' = \mu\frac{du}{dy} \tag{9}$$

In Eq. (8), the slip length coefficient β, is carried through the derivation for completeness, though later set to zero to produce a no-slip condition. The second boundary condition, Eq. (9), captures the Marangoni effects at the free liquid-vapour interface. Integrating Eq. (7), the thin-film liquid velocity is obtained as a function of the liquid pressure and interfacial temperature gradients.

$$u = \frac{1}{\mu}\frac{dP_l}{dx}\left(\frac{y^2}{2} - \delta(y-\beta)\right) + \frac{b}{\mu}\frac{dT_{lv}}{dx}(y-\beta) \tag{10}$$

With the velocity of the liquid in the thin film described by Eq. (10), the mass flow rate can be obtained through the application of continuity. After integrating over the film thickness, the mass flow rate at any point along the thin film is obtained as,

$$\dot{m} = \frac{1}{\nu}\frac{dP_l}{dx}\left(-\frac{\delta^3}{3} + \beta\delta^2\right) + \frac{b}{\nu}\frac{dT_{lv}}{dx}\left(\frac{\delta^2}{2} - \beta\delta\right) \tag{11}$$

The temperature of the channel walls is assumed be constant and uniform with heat being conducted through the film thickness normal to the planar wall. Reflecting this, the energy equation and boundary conditions take the following form,

$$\frac{\partial}{\partial y}\left(k_l\frac{\partial T}{\partial y}\right) = 0 \tag{12}$$

At $y = 0$,

$$T = T_w \tag{13}$$

At $y = \delta$,

$$-k_l\frac{\partial T}{\partial y} = \dot{m}''h_{fg} \tag{14}$$

Integrating the energy equation, Eq. (12), and applying the appropriate boundary conditions, Eqs. (13) and (14), an expression for the evaporative mass flux is obtained.

$$\dot{m}'' = \frac{k_l(T_w - T_{lv})}{\delta h_{fg}} \tag{15}$$

The evaporative mass flux can be related to the liquid mass flow by,

$$\dot{m}'' = -\frac{d\dot{m}''}{dx} \tag{16}$$

Integrating Eq. (16) with respect to film length x, the mass flow rate in the thin film is described as,

$$\dot{m} = -\int_0^x \frac{k_l(T_w - T_{lv})}{\delta h_{fg}}dx \tag{17}$$

From Eqs. (11) and (17), a relation between the liquid pressure gradient and interfacial temperature gradient is obtained.

$$\frac{dP_l}{dx} = b\frac{C_5}{C_4}\frac{dT_{lv}}{dx} + \frac{\nu k_l}{C_4 h_{fg}}\int_0^x \frac{T_w - T_{lv}}{\delta}dx \tag{18}$$

where,

$$C_4 = \frac{\delta^3}{3} - \beta\delta^2 \tag{19}$$

$$C_5 = \frac{\delta^2}{2} - \beta\delta \tag{20}$$

To form a closed solution to the governing equation, the Kelvin-Clapeyron evaporation model, introduced by Wayner Jr. (Wayner Jr., 1991), is used.

$$\dot{m}'' = \frac{1}{h_{fg}}\left(h_{lv}^{cl}(T_{lv} - T_v) - h_{lv}^{kl}(P_d + P_c)\right) \tag{21}$$

$$h_{lv}^{cl} = \eta\left(\frac{1}{T_{lv}}\right)^{3/2}\left(\frac{Mh_{fg}}{T_v}\right) \tag{22}$$

$$h_{lv}^{kl} = \eta\left(\frac{1}{T_{lv}}\right)^{3/2}V_l \tag{23}$$

$$\eta = \left(\frac{C^2M}{2\pi R}\right)^{1/2}\left(\frac{P_v h_{fg}}{R}\right) \tag{24}$$

$$C = \frac{2\gamma}{2-\gamma} \tag{25}$$

By equating the evaporative mass flux expressions, Eqs. (15) and (21), a relation is obtained where the interfacial temperature is described independently of the liquid pressure. Differentiating with respect to the thin-film length *x*, the interfacial temperature gradient is obtained as follows:

DOI: 10.5098/hmt.v4.1.3002 ISSN: 2151-8629

$$\frac{dT_{lv}}{dx} = \frac{2T_v}{\delta^3}\left(\frac{\chi + V_l\eta\sigma\delta^4\kappa'}{\omega}\right) \quad (26)$$

where,

$$\chi = \delta'\left[k_l\delta^2\left(T_{lv}^{5/2} - T_wT_{lv}^{3/2}\right) - 3AV_l\eta\right] \quad (27)$$

$$\omega = k_lT_v\left(5T_{lv}^{3/2} - 3T_wT_{lv}^{1/2}\right) + 2\delta\eta\left(Mh_{fg} - V_lT_vb\kappa\right) \quad (28)$$

Collecting Eqs. (6, 18, 26) and rearranging for δ''', the governing equation for the evaporating thin film is described as,

$$\delta''' = \frac{3\delta'\delta''^2}{\alpha} - \left(\frac{\omega\alpha^{\frac{3}{2}}}{\omega\alpha^{3/2} + 2T_v\psi V_l\eta\sigma\delta}\right)\left[\frac{2T_v\psi\chi}{\omega\delta^3} - \frac{\alpha^{\frac{3}{2}}}{\sigma}\left(\frac{3A}{\delta^4}\delta' - \frac{\nu k_l}{C_4h_{fg}}\int_0^x\frac{T_w - T_{lv}}{\delta}dx\right)\right] \quad (29)$$

where,

$$\psi = \frac{b}{\sigma}\left(\frac{C_5}{C_4}\alpha^{3/2} + \delta''\right) \quad (30)$$

Thus, the governing equation is obtained as a function of film thickness and associated derivatives, fluid properties and the interfacial temperature.

2.1 Initial conditions and limitations

To obtain the adsorbed film thickness, it is assumed that no evaporation is taking place in the adsorbed region. Thus, the evaporative mass flux from the Kelvin-Clapeyron model, Eq. (21), is set to zero and the interfacial temperature is assumed to be that of the wall in the adsorbed region. This yields the following equation for the adsorbed film thickness.

$$\delta_0 = \left[\frac{AV_l}{Mh_{fg}}\left(\frac{T_v}{T_w - T_v}\right)\right]^{1/3} \quad (31)$$

As it was discussed previously, to avoid a trivial solution of constant thin film thickness, small perturbations need to be applied to the initial conditions (δ, δ' and δ''). As a goal to obtain accurate solutions for thin-film region, the perturbations must be sufficiently small to ensure proximity to the adsorbed region as perturbations serve to effectively shift the coordinate system away from the adsorbed region. To avoid violating the evaporative mass flux balance, the possible limits of important parameters are searched. Thus, a maximum and minimum value range for δ'' is obtained as a function of δ and δ'.

On the lower end of the perturbation applied to δ'', the replacement of the interfacial temperature with that of the vapour temperature gives

$$\delta''_{min} = -\alpha^{3/2}\left[\frac{k_l(T_w - T_v)}{V_l\sigma\delta\eta}T_v^{3/2} + \frac{P_d}{\sigma}\right] \quad (32)$$

Upon inspection, it is seen that $\delta''_{min} < 0$ for all cases. Thus, it is imposed that the minimum value be set to $\delta''_{min} > 0$, so as to ensure a non-trivial solution of monotonically increasing film thickness.

Conversely, the upper bound for δ'' is obtained by equating the interfacial temperature to that of the wall temperature. Solving for δ''_{max},

$$\delta''_{max} = \frac{\alpha^{3/2}}{\sigma}\left(\frac{Mh_{fg}}{T_vV_l}(T_w - T_v) - P_d\right) \quad (33)$$

Inspecting Eq. (33), it is observed that the following inequality must be satisfied so as to ensure a monotonic increase in thin film thickness.

$$\frac{Mh_{fg}}{T_vV_l}(T_w - T_v) \geq \frac{A}{\delta^3} \quad (34)$$

Thus, only solutions satisfying the aforementioned perturbation limits are valid. A check must be performed when specifying the initial conditions so as to avoid any inadvertent violations of the mass flux balance or assumptions made in the analysis.

3. NUMERICAL SOLUTION PROCEDURE

The governing equation, Eq. (29), is solved with the use of a Runge-Kutta RK5 (4) 7M method, as proposed by Dormand and Prince (1980). The RK5 (4) 7M method is a modified 5th order technique designed to produce small principal truncation terms. The solution procedure is iterative. At a given solution step, the integral term contained in Eq. (29), $\int_0^x\frac{T_w - T_{lv}}{\delta}dx$, needs to be solved, which requires the knowledge of the current film thickness and interfacial temperature. These values are unknown at the current position step and need to be guessed. As a first guess, the values from the previous step are used, and the calculated values are returned from the Runge-Kutta solver and compared to the guess values. A comparison of the guess and calculated values is performed and looped until convergence criteria for both film thickness, Eq. (35) and interfacial temperature Eq. (36), are satisfied. The numerical solver is coded in MATLAB, and follows the simplified flowchart shown in Fig. 2.

$$\left|\frac{\delta_{guess} - \delta_{solved}}{\delta_{solved}}\right| \leq 0.1\% \quad (35)$$

$$\left|\frac{T_{lv_{guess}} - T_{lv_{solved}}}{T_{lv_{solved}}}\right| \leq 0.1\% \quad (36)$$

The code solves the governing equation and returns a solution when the far field curvature of the thin film has achieved the constant curvature convergence criteria (±0.01 %). The code terminates when the convergence criteria for constant curvature has been satisfied for ten consecutive steps. Though a constant curvature solution may be obtained, the desired curvature of Young-Laplace ($1/H$) is sought. Thus, an upper and lower bound are searched out, after which the search is completed by algorithm until the desired far field constant curvature condition ($\kappa = 1/H \pm 0.01\%$) is achieved. Due to the highly non-linear nature of the governing equation and the convergence criteria (±0.01 %), the perturbation value (ε_2), required a case specific precision as denoted in Table 2.

4. RESULTS AND DISCUSSION

A typical set of results obtained for pentane in a channel of 20 μm width and superheats of ($T_w - T_v$)= 0.01 K and 0.1 K at T_v= 300 K is presented in Fig. 3. This type of behaviour is representative of the thin-film development observed in other previous works, for example in Wee et al. (2005). Similarly, it is found that the numerical solution is very sensitive to the initial conditions and applied perturbations. Specifically, the results were extremely sensitive to the value of δ' and its associated perturbation ε_2. Increasing the superheats effectively steepens the thin-film profile and decreases the thin-film length. As a result of the thin-film geometry, the perturbation magnitude and sensitivity increases at larger superheats. In our solutions, we found that ε_1 had to be increased in order to seek an appropriate ε_2. However, it should be noted that applied perturbations must be sufficiently small such as to not shift the origin of the

Global Digital Central
ISSN: 2151-8629

coordinate system too far into the thin-film region. A large perturbation may lead to exclusion of the near adsorbed region and thus the loss of important information for the entire solution.

Figure 4 provides a comparison to the thin-film profile generated in this study to that of Wang et al. (2007), where the thickness perturbation ε_1, was provided for one of the cases presented. Observing Fig. 4, it is seen that the profiles have the same general trend. It is of note that Wang et al. (2007) used a 4th order ODE as opposed to the 3rd order used in this study. In the 4th order model, the main sensitivity lies on the perturbation on $\delta''(\varepsilon_3)$, which needs to be iteratively determined. In a 3rd order model, the sensitivity falls on the slope perturbation, $\delta'(\varepsilon_2)$, which was determined by the numerical model to match the far field boundary condition. In the 4th order model, the slope perturbation is not sensitive so $\delta' = 1\times10^{-11}$ was used in Wang et al. (2007). In our case, the solutions were not sensitive to δ'' so it was set at 1×10^{-3}. Note that the evaporation models were also different between Wang et al. (2007) and the work presented here.

In many other works, the perturbations used are not provided. As a result, a direct comparison was not possible. Table 2 provides a list of parameters used in generating the solutions including the applied perturbations to Figs. 3 and 4 so that the future works can be directly compared against our work.

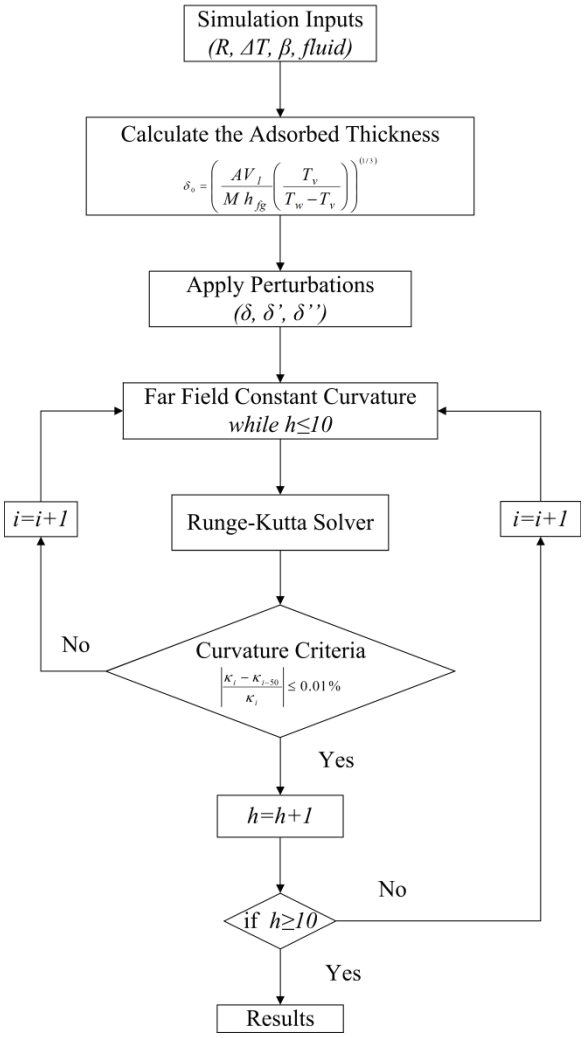

Fig. 2 Simplified flowchart outlining the solution procedure.

Table 2 Input parameters used in generating thin-film solutions.

Input	Fig. 3	Fig. 4
Fluid	Pentane	Octane
Superheat	0.01 K, 0.1 K	1 K
$2H$	20 μm	5 μm
T_V	300 K	343 K
$\delta_{0@0.01\,K}$	$4.68376868475136\times10^{-9}$ m	1.70×10^{-3} m
$\delta_{0@0.1\,K}$	$2.950758143324543\times10^{-9}$ m	
ε_1	$\delta_0 \times 0.01\%$ m	1.70×10^{-3} m
$\varepsilon_{2@0.01\,K}$	2.5205788×10^{-6}	1.477109375×10^{-2}
$\varepsilon_{2@0.1\,K}$	$2.637589900102466\times10^{-6}$	
ε_3	1×10^{-3} m^{-1}	1×10^{-3} m^{-1}
ε_4	0	0

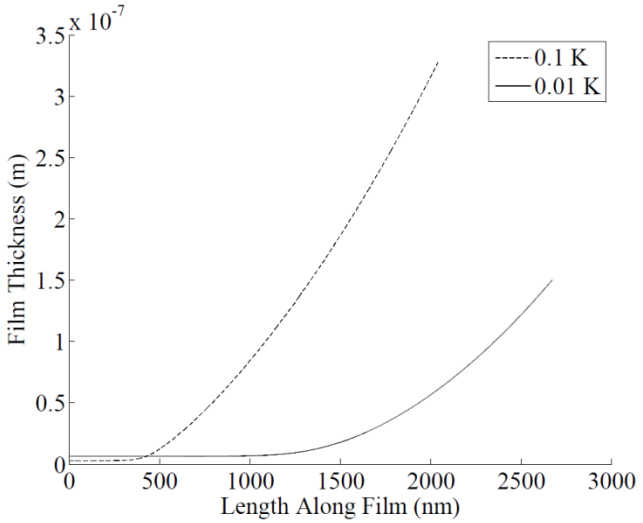

Fig. 3 Thin-film profile of pentane in a channel of 20 μm width at different superheats.

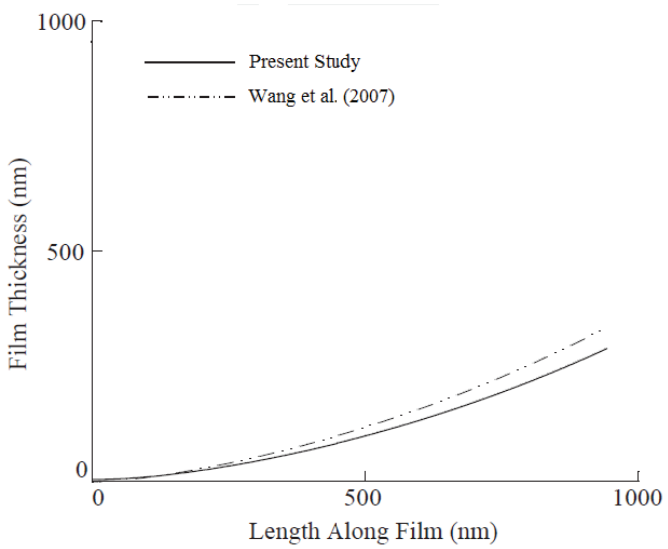

Fig. 4 Thin-film profile comparison to Wang et al. (2007).

DOI: 10.5098/hmt.v4.1.3002 ISSN: 2151-8629

4.1 Accommodation coefficient

The variable γ in Eq. (25) represents the accommodation coefficient. The accommodation coefficient is often used as unity in majority of the previouslsy published works: Wang et al. (2007); Wee et al. (2005); Qu et al. (2002); Schonberg et al. (1995); Stephan et al. (1992), without much discussion. An accommodation coefficient of unity implies that for every liquid molecule emitted, none are rebounded and re-absorbed, giving a perfect evaporative capacity. Mills (1965) notes that in cases of extreme fluid purity, this value should tend to unity. However, extreme purity may be unrealistic to obtain, as such the value should be lower than unity.

The effect of the accommodation coefficient is mostly omitted in the previously published thin-film solutions, yet in the case of numerically modelling a thin-film meniscus, alters the results noticeably. In some works, Wee et al. (2005); Du and Zhao (2011), $C = 2\gamma/(2-\gamma)$ was defined as accommodation coefficient and a value of 2.0 was assigned to C, resulting in the true accommodation coefficient, γ = 1.0. Panchamgam et al. (2008) referred to this C as the constant of proportionality. Thus, there is an ambiguity in the general use of this term.

Figure 5 demonstrates how the thin-film profile alters with decreasing accommodation coefficient. This analysis was performed with pentane as the working fluid in a 20 μm channel and a 0.01 K superheat. It is clear that with a decreasing value of accommodation coefficient, the film growth is delayed, resulting in a longer thin film and consequently a modified thin-film interface shape. This result was expected as a smaller accommodation coefficient would suggest less evaporative mass flux, thus extending adsorbed region of the film. The seemingly abrupt end of the thin-film profiles for γ = 0.4 and γ = 0.3 was due to the constant curvature termination condition. At these lower values of accommodation coefficient, the curvature profile loses the associated overshoot, as shown in Fig. 6.

Evaporative mass flux can be seen in Fig. 7 with decreasing accommodation coefficient. Not only does the peak magnitude of mass flux decrease, but the location is shifted along the length of the film. This corresponds with the extension of the thin-film profiles, thus the disjoining pressure decrease is retarded along the length of the film.

Observing the end of the evaporative mass flux profiles, it is clear in all cases, that evaporative mass flux at the constant curvature condition is non-zero. As mentioned earlier this deals with the use of the augmented Young-Laplace equation which entails some residual mass flux towards the intrinsic meniscus. In addition, retarding the evaporation by implementing a lower value of accommodation coefficient leaves an increased residual mass flux in order to satisfy the mass flux balance used in the derivation.

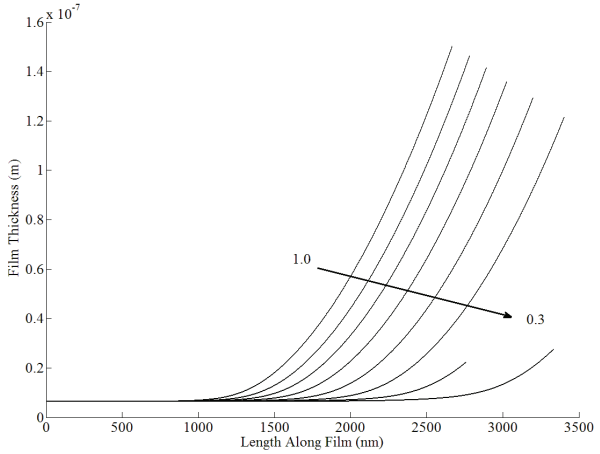

Fig. 5 Effect of accommodation coefficient on thin-film profile (Results presented in decrements of 0.1 from γ =1.0 to 0.3).

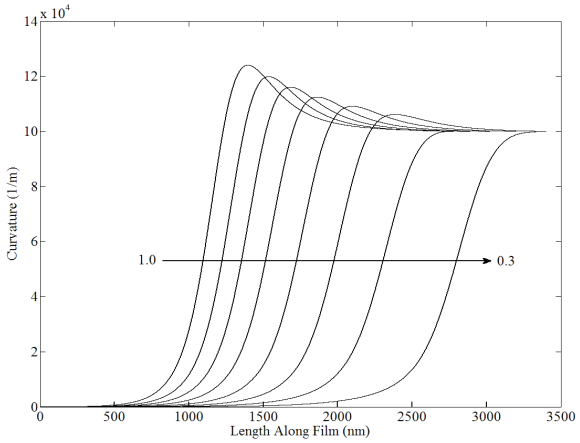

Fig. 6 Effect of accommodation coefficient on curvature (Results presented in decrements of 0.1 from γ =1.0 to 0.3).

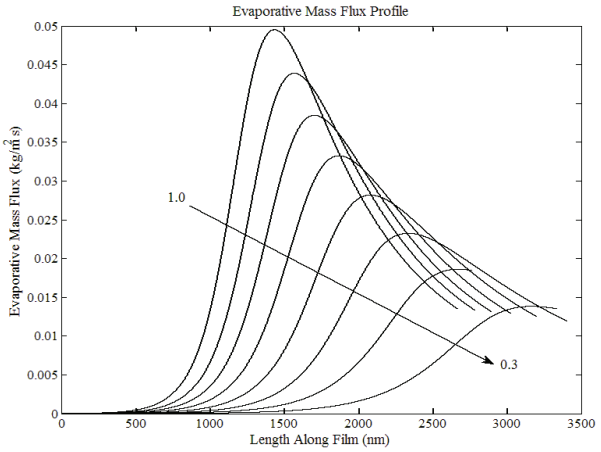

Fig. 7 Effect of accommodation coefficient on evaporative mass flux (Results presented in decrements of 0.1 from γ =1.0 to 0.3).

From these plots it is clear that altering the accommodation coefficient does indeed have a significant effect on the evaporative characteristics of the thin film.

It should be noted that the origin of the coordinate system is arbitrary for the shooting techniques used in this work. However, when the accommodation coefficient was varied not only the origin but also the overall shape of the solutions was also altered. As a result, without sufficient knowledge of accommodation coefficient, results are at best qualitative.

4.2 Hamaker constant

A similar ambiguity exists for the Hamaker constant, which had been estimated by using different methods. A survey of thin film works indicates a range of values were used for differing arrangements. This can be attributed to the many different relations proposed to estimate the Hamaker constant value for a given set of materials.

In our analysis, the Tabor-Winterton approximation is used to obtain a value for the Hamaker constant as outlined in Butt and Kapl (2010), and Israelachvili (1991). In this method, the Hamaker constant for the solid-liquid-vapour system (132) is given as a function of temperature, absorption frequency, index of refraction and dielectric constant by the following equation,

Global Digital Central
ISSN: 2151-8629

$$A_H = A_{132} = k_B T \left(\frac{\xi_1 - \xi_3}{\xi_1 + \xi_3}\right)\left(\frac{\xi_2 - \xi_3}{\xi_2 + \xi_3}\right)\frac{3}{4} + \frac{3h\nu_e}{8\sqrt{2}} \times$$

$$\frac{(n_1^2 - n_3^2)(n_2^2 - n_3^2)}{(n_1^2 + n_3^2)^{1/2}(n_2^2 + n_3^2)^{1/2}\{(n_1^2 + n_3^2)^{1/2} + (n_2^2 + n_3^2)^{1/2}\}} \quad (37)$$

Of the functional terms in Eq. (37), the absorption frequency for the working fluid, ν_e, comes into question, as more than one absorption peak exists for any given material, or combination of materials. As a result of this uncertainty, a parametric study was conducted to determine the effect of variability in the Hamaker constant on the thin-film profile. By using an absorption frequency value of ν_e = 1.7635×10^{15} Hz from Costner et al. (2009), the dispersion constant was calculated to be A = 2.013×10^{-21} J using Eq. (37), which was consistent with the values provided in Israelachvili (1991).

For the parametric study, the dispersion constant was set for a range of values around the calculated dispersion constant (1×10^{-21} ≤ A ≤ 10×10^{-21}) in an effort to illustrate its effect on the thin-film profile and evaporation. The geometry of the thin film, as shown in Fig. 8, illustrates that an increasing dispersion constant results in a thickening of the adsorbed layer and an elongation of the thin film length.

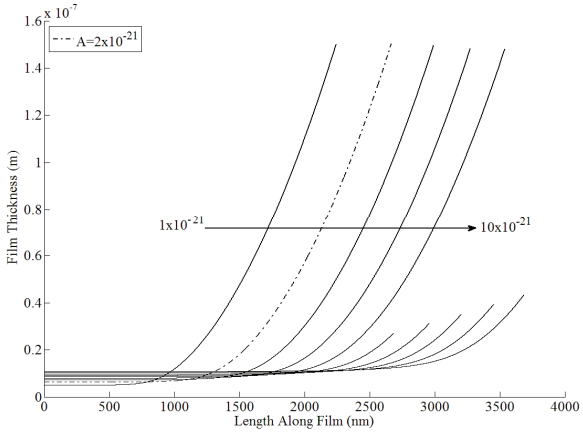

Fig. 8 Thin film profiles for increasing dispersion constants in increments of 1×10^{-21}.

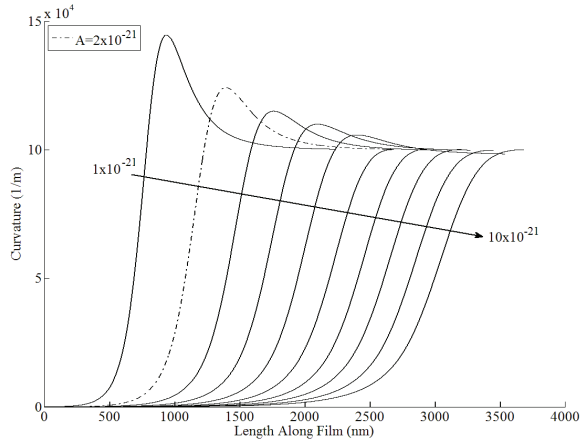

Fig. 9 Local curvature profiles for increasing dispersion constants in increments of 1×10^{-21}.

It is important to note that the thin-film termination location changes significantly for higher values of the dispersion constant. This termination can be explained by the reduction in the local curvature overshoot with increasing dispersion constant, shown in Fig. 9, similar to the trend observed previously in Fig. 6. Thus it is evident, that changes in the dispersion constant can significantly affect the thin film profile and evaporation capacity. In regards to evaporation, it can be seen in Fig. 10 that the peak evaporation rate decreases slightly with increasing dispersion constant.

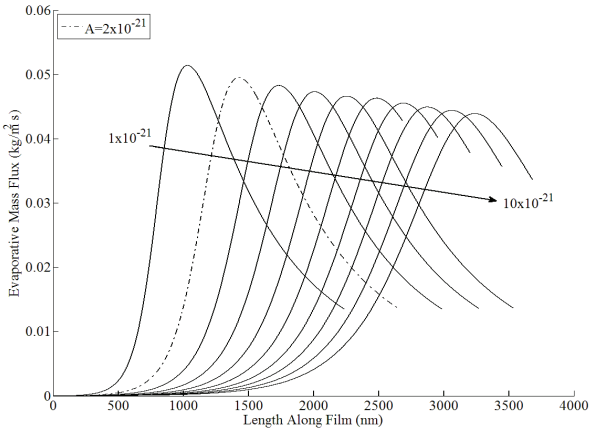

Fig. 10 Evaporative mass flux in the thin film region with increasing dispersion values in increments of 1×10^{-21}.

4.3 Absolute negative liquid pressure

At higher superheats, near the adsorbed region, disjoining effects are so pronounced that in satisfying the force-balance, Eq. (1), an absolute negative liquid pressure is generated. In the previously published thin-film solutions, the absolute negative liquid pressures were not explicitly discussed. For example, in Wang et al. (2007), a liquid pressure change (ΔP) was defined with respect to the pressure obtained in the assumed starting point of the thin-film solution instead of plotting the liquid pressure directly. Figure 11 shows a composite pressure profile at T_v = 300 K for a 1 K superheat, a channel width of 5 μm, and octane as the working fluid. The absolute negative liquid pressure inside the thin-film can be clearly seen in Fig. 11. As the film thickness decreases, the disjoining pressure quickly increases, leading to a decrease in the liquid pressure. For very thin films, the liquid pressure becomes negative to satisfy Eqs. (1) and (2).

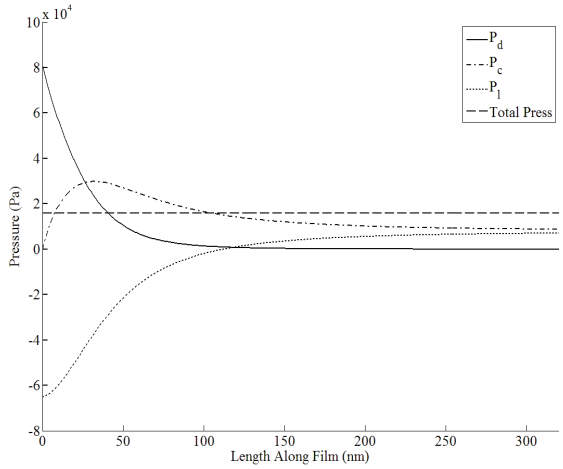

Fig. 11 Composite pressure profile for 1 K superheat, a channel width of 5 μm, and octane as the working fluid.

Global Digital Central
ISSN: 2151-8629

Maroo and Chung (2010) also reported a negative absolute liquid pressure in their analysis of evaporating meniscus using molecular dynamics. They speculated that this negative liquid pressure occurs in regions where the liquid film is being pulled by the relatively cooler liquid in the meniscus, and also towards the centre due to high disjoining pressure. The negative liquid pressures, where liquid is in a highly unstable state of tension, have been previously experimentally observed as explained in Batchelor (1979). It is possible that thin films can sustain negative pressures as the film thickness can be smaller than the critical cavitation radius. However, it is open to debate whether the negative liquid pressure originates from the simplified nature of the thin-film mathematical model or the model correctly predicts the liquid pressure in a thin film.

5. CONCLUSIONS

The non-linear ODE representing the evaporating thin film in a channel was numerically solved and the results were discusses in detail. A summary of the fundamental findings are as follows:

The numerical solution is very sensitive to the initial conditions and the applied perturbations. In particular extreme sensitivity was found with the applied value of $\delta'$and its associated perturbation ε_2. In addition, applied perturbations must be small enough such as to not shift the origin of the coordinate system to far into the thin-film region. Using too large of perturbations can result in omission of key attributes near the adsorbed region.

The accommodation coefficient and Hamaker constant had a pronounced effect on thin-film geometry and associated characteristics. Although the starting point of the solution is subject to an arbitrary shift due to the shooting techniques used, it is clear that varying these coefficients affect not only the origin but also overall shape of the resulting profiles.

Decreasing accommodation coefficient shallowed the thin-film profile. This shallowing resulted in a retardation of the decline in disjoining pressure. This corresponded in delaying the increase in liquid pressure and shifting the peak evaporative mass flux along the length of the film. The magnitude in evaporative mass flux also decreased with decreasing accommodation coefficient. Curvature overshoot was also observed to diminish with decreasing accommodation coefficient.

The variance in the Hamaker constant modified the profiles and physical characteristics of the thin film. As the Hamaker constant was increased, the thin-film length was extended, the peak evaporative mass flux was shifted towards the intrinsic meniscus, and the evaporative mass flux magnitude decreased.

Disjoining pressure effects are much more pronounced near the adsorbed layer, creating absolute negative liquid pressures. The thin films can theoretically sustain negative liquid pressures due to their small thicknesses. However, without experimental validation, the presence of negative pressures in thin films remains controversial.

It is important to highlight that from the above analyses, the current results of thin-film studies are very significant in gaining insight into the heat transfer characteristics of an evaporating thin-film. However, with the above inconsistencies identified, results can only be regarded as qualitative trends. With the ambiguity that exists within these parameters such as accommodation coefficient, Hamaker constant and applied perturbations, experimental investigation is necessary to verify the numerical results.

ACKNOWLEDGEMENTS

The support from Natural Sciences and Engineering Research Council of Canada under Discovery Grants Program is greatly appreciated.

NOMENCLATURE

a	Surface tension coefficient (N/m)
A	Dispersion constant (J)
A_H, A_{132}	Hamaker constant (J)
b	Surface tension temperature coefficient (N/m·K)
C	Constant of proportionality
C_4	Slip length relation coeff (m^3)
C_5	Slip length relation coeff (m^2)
Ca	Capillary number
h	Plank's constant (J·s)
h_{fg}	Latent heat of vapourization (J/kg·K)
h_{lv}^{cl}	Clapeyron evaporative mass flux coeff (kg/m^2·s·K)
h_{lv}^{kl}	Kelvin evaporative mass flux coeff (s/m)
H	Channel height (m)
k_l	Liquid conductivity (W/m·K)
k_B	Boltzmann's constant (J/s·m^2·K^4)
$\dot{m}$	Mass flow rate (kg/s)
$\dot{m}''$	Evaporative mass flux (kg/m^2·s)
M	Molecular mass (kg/kmol)
n	Index of refraction
P	Pressure (N/m^2)
R	Universal gas constant (J/mol·K)
T	Temperature (K)
u	Axial velocity (m/s)
V_l	Molar volume (m^3/mol)
V	Liquid velocity (m/s)
x	x direction (m)
y	y direction (m)

Greek symbols

α	Local curvature term
β	Wall slip length (m)
γ	Accommodation coefficient
δ	Thin film thickness (m)
ε_1	Thickness perturbation (m)
ε_2	Slope perturbation
ε_3	Perturbation applied to δ'' (1/m)
η	Kelvin-Clapeyron mass flux coeff (mol·$K^{3/2}$/s·m^2)
κ	Local curvature (1/m)
μ	Dynamic viscosity (Pa·s)
ν	Kinematic viscosity (m^2·s)
ν_e	Main absorption frequency (1/s)
ξ	Dielectric constant
σ	Surface tension (N/m)
τ	Liquid-vapour interfacial shear stress (N/m^2)
χ	Collection of terms in ODE (W·m·$K^{3/2}$)
ψ	Collection of terms in ODE (1/m·K)
ω	Collection of terms in ODE (W·$K^{3/2}$/m)

Subscripts

c	Capillary
d	Disjoining
l	Liquid
lv	Liquid-vapour interface
v	Vapour
w	Wall

REFERENCES

Batchelor, G.K., 1979, *An introduction to Fluid Dynamics*, Cambridge University Press, New York

Butt, Hans-Jurgen and Kappl, Michael, 2010, *Surface and Interfacial Forces*, Wiley-VCH Verlag GmbH & Co. KGaA

Costner, E.A., Long, K.B., Navar, C., Jockusch, S., Lei, X., Zimmerman, P., Campion, A., Turro, N.J., Willson, C.G., 2009,

"Fundamental Optical Properties of Linear and Cyclic Alkanes: VUV Absorbance and Index of Refraction," *Journal of Physical Chemistry*, **113**(33), 9337-9347
http://dx.doi.org/10.1021/jp903435c

DasGupta, S., Kim, I.Y., Wayner Jr.,P.C., 1994, "Use of the Kelvin-Clapeyron Equation to Model an Evaporating Curved Microfilm," *Journal of Heat Transfer*, **116**(4), 1007-1014
http://dx.doi.org/10.1115/1.2911436

DasGupta, S., Schonberg, J.A., Kim, I.Y., Wayner Jr., P.C., 1993, "Use of the Augmented Young-Laplace Equation to Model Equilibrium and Evaporating Extended Menisci," *Journal of Colloid and Interface Science*, **157**(2), 332-342
http://dx.doi.org/10.1006/jcis.1993.1194

Dormand, J.R. and Prince, P.J., 1980, "A Family of Embedded Runge-Kutta Formulae," *Journal of Computational and Applied Mathematics* **6**(1), 19-26
http://dx.doi.org/10.1016/0771-050X(80)90013-3

Du, S.-Y. and Zhao, Y.-H., 2011, "New Boundary Conditions for the Evaporating Thin-Film Model in a Rectangular Micro Channel," *International Journal of Heat and Mass Transfer*, **54**(15-16)**,** 3694-3701
http://dx.doi.org/10.1016/j.ijheatmasstransfer.2011.02.059

Du, S.-Y. and Zhao, Y.-H., 2012, "Numerical Study of Conjugated Heat Transfer in Evaporating Thin-films Near The Contact Line," *International Journal of Heat and Mass Transfer*, **55**(1-3), 61-69
http://dx.doi.org/10.1016/j.ijheatmasstransfer.2011.08.039

Hallinan, K.P., Kim, S.J., Chang, W.S., 1994, "Evaporation from an Extended Meniscus for Nonisothermal Interfacial Conditions," *Journal of Thermophysics and Heat Transfer*, **8**(4), 709-716
http://dx.doi.org/10.2514/3.602

Israelachvili, Jacob, 1991, *Intermolecular and Surface Forces*, Academic press Harcourt Brace Jovanovich Publishers, Toronto

Kou, M.L. and Bai, Z.H., 2011, "Effects of Wall Slip and Temperature Jump on Heat and Mass Transfer Characteristics of an Evaporating Thin Film," *International Communications in Heat and Mass Transfer*, **38**(7)**,** 874-878.
http://dx.doi.org/10.1016/j.icheatmasstransfer.2011.03.032

Maroo, S.C. and Chung, J.N., 2010, "Heat Transfer Characteristics and Pressure Variation in a Nanoscale Evaporating Meniscus," *International Journal of Heat and Mass Transfer*, **53**(15-16), 3335-3345
http://dx.doi.org/10.1016/j.ijheatmasstransfer.2010.02.030

Mills, A. F., 1965, "The Condensation of Steam at Low Pressures," *Technical Report on NSF GP-2250*, **6**(9), Space Sciences Laboratory, University of California at Berkley

Moosman, S. and Homsy, G.M., 1980, "Evaporating Menisci of Wetting Fluids," *Journal of Colloid and Interface Science*, 73(1), 212-223.
http://dx.doi.org/10.1016/0021-9797(80)90138-1

Morris, S. J. S., 2003, "The Evaporating Meniscus in a Channel," *Journal of Fluid Mechanics*, **494**, 297-317.
http://dx.doi.org/10.1017/S0022112003006153

Panchamgam, S.S., Chatterjee, A., Plawsky, J.L., Wayner Jr., P.C., 2008, "Comprehensive Experimental and Theoretical Study of Fluid Flow and Heat Transfer in a Microscopic Evaporating Meniscus in a Miniature Heat Exchanger," *International Journal of Heat and Mass Transfer*, **51**(21-22), 5368-5379
http://dx.doi.org/10.1016/j.ijheatmasstransfer.2008.03.023

Park, K. and Lee, K.-S., 2003, "Flow and Heat Transfer Characteristics of the Evaporating Extended Meniscus in a Micro-Capillary Channel," *International Journal of Heat and Mass Transfer*, **46**(24), 4587-4594
http://dx.doi.org/10.1016/S0017-9310(03)00306-5

Park, K., Noh, K.J., Lee, K.S., 2003, "Transport Phenomena in the Thin-Film Region of a Micro-Channel," *International Journal of Heat and Mass Transfer*, **46**(13), 2381-2388
http://dx.doi.org/10.1016/S0017-9310(02)00541-0

Potash Jr., M. and Wayner Jr., P.C., 1972, "Evaporation from a Two-Dimensional Extended Meniscus," *International Journal of Heat and Mass Transfer*, **15**(10), 1851-1863
http://dx.doi.org/10.1016/0017-9310(72)90058-0

Qu, W., Ma, T., Miao, J., Wang, J., 2002, "Effects of Radius and Heat Transfer on the Profile of Evaporating Thin Liquid Film and Meniscus in Capillary Tubes," *International Journal of Heat and Mass Transfer*, **45**(9), 1879-1887
http://dx.doi.org/10.1016/S0017-9310(01)00296-4

Schonberg, J. A., DasGupta, S., Wayner Jr., P.C., 1995, "An Augmented Young-Laplace Model of an Evaporating Meniscus in a Microchannel with High Heat Flux," *Experimental Thermal and Fluid Science*, **10**(2), 163-170
http://dx.doi.org/10.1016/0894-1777(94)00085-M

Stephan, P.C. and Busse, C.A., 1992, "Analysis of the Heat Transfer Coefficient of Grooved Heat Pipe Evaporator Walls," *International Journal of Heat and Mass Transfer*, **35**(2), 383-391
http://dx.doi.org/10.1016/0017-9310(92)90276-X

Wang, H., Garimella, S.V., Murthy, J.Y., 2008, "An Analytical Solution for the Total Heat Transfer in the Thin-Film Region of an Evaporating Meniscus," *International Journal of Heat and Mass Transfer*, **51**(25-26), 6317-6322
http://dx.doi.org/10.1016/j.ijheatmasstransfer.2008.06.011

Wang, H., Garimella, S.V., Murthy, J.Y., 2007, "Characteristics of an Evaporating Thin Film in a Microchannel," *International Journal of Heat and Mass Transfer*, **50**(19-20), 3933-3942
http://dx.doi.org/10.1016/j.ijheatmasstransfer.2007.01.052

Wayner Jr., P.C., Kao, Y.K., LaCroix, L.V., 1976, "The Interline Heat-Transfer Coefficient of an Evaporating Wetting Film," *International Journal of Heat and Mass Transfer*, **19**(5), 487-492
http://dx.doi.org/10.1016/0017-9310(76)90161-7

Wayner Jr., Peter C., 1991, "The Effect of Interfacial Mass Transport on Flow in Thin Liquid Films," *Colloids and Surfaces*, **52**, 71-84
http://dx.doi.org/10.1016/0166-6622(91)80006-A

Wee S.-K., Kihm, K.D., Hallinan, K.P., 2005, "Effects of the Liquid Polarity and the Wall Slip on the Heat and Mass Transport Characteristics of the Micro-Scale Evaporating Transition Film," *International Journal of Heat and Mass Transfer*, **48**(2), 265-278
http://dx.doi.org/10.1016/j.ijheatmasstransfer.2004.08.021

Zhao, J.-J., Duan, Y.Y., Wang, X.D., Wang, B.X., 2011, "Effects of Superheat and Temperature-Dependent Thermophysical Properties on Evaporating Thin Liquid Films in Microchannels," *International Journal of Heat and Mass Transfer*, **54**(5-6), 1259-1267
http://dx.doi.org/10.1016/j.ijheatmasstransfer.2010.10.026